

# Evaluation of the effects of direct solar radiation on fiber-based distributed temperature sensing

Zhizhi Yang<sup>a</sup>, Pieter Sanczuk<sup>b</sup>, Louise Terryn<sup>b</sup>, Pieter De Frenne<sup>b</sup>, Hans Verbeeck<sup>b</sup>, Emma Van de Walle<sup>b</sup>, Kim Calders<sup>b</sup>, Bart Kuyken<sup>a</sup>, Roel Baets<sup>a</sup>, and Yanlu Li<sup>a</sup>

<sup>a</sup>Photonics Research Group, Department of Information Technology, Faculty of Engineering and Architecture, Ghent University-Imec, Ghent, Belgium; <sup>b</sup>Q-ForestLab, Department of Environment, Faculty of Bioscience Engineering, Ghent University, Belgium

## ABSTRACT

Accurate and precise measurements of microclimatic temperatures are important for understanding microclimate dynamics within forests, which are crucial in the face of climate change. Various methods exist for measuring microclimate temperatures in the field; however, for ultra-high-resolution measurements in space (< 1 m) and time (< 1 minute), optical fiber-based sensing systems become a promising option. Specifically, a Distributed Temperature Sensing (DTS) system coupled with a fiber over 100 – 1000 m long could be highly suitable to collect spatial temperature data continuously in forests and other vegetation types. Although DTS is accurate in controlled lab conditions, the impacts of environmental factors such as energy fluxes from direct solar radiation on temperature measurements remain to be quantified. Given the environmental variability in forest ecosystems, it is essential to take into account the increase in fiber temperatures due to solar radiation.

Here we explore the impact of radiative fluxes from direct sunlight on the optical fibers used in DTS systems. To evaluate the impact of radiative fluxes on the thermal accuracy of a DTS, we conducted a field experiment with direct solar radiation. We put two fiber regions under the same condition, but one region is coated with aluminum while the other one is uncoated.

We observed distinct thermal responses between aluminum-coated and uncoated sections of the optical fibers when exposed to solar radiation, with the uncoated fiber exhibiting a higher temperature under the same conditions. Our results can be used to mitigate this bias in field measurements, enhancing the accuracy of DTS in environmental monitoring, and deepening our understanding of the effects of solar radiation on fiber-based remote sensing technologies.

**Keywords:** Air temperature, ecology, microclimate, Distributed Temperature Sensing, remote sensing, optical fiber.

## 1. INTRODUCTION

Accurate measurement of microclimatic temperatures is important for understanding microclimate dynamics within forests [1]. Traditionally, discrete temperature sensors are limited to several certain locations, making them uneconomical for a large area data collection [2, 3]. To realize an ultra-high-resolution measurement in space (< 1 m) and time (< 1 minute), optical fiber-based distributed sensing constitutes a promising alternative. Distributed Temperature Sensing (DTS) system coupled with a fiber over a kilometer long could be highly suitable to collect spatial temperature data quasi-continuously in space and over time. Yet, the application of DTS in ecological settings remains rarely done.

Although measuring ambient air temperatures using DTS is accurate in controlled lab conditions, the impacts of environmental factors such as radiation fluxes from direct solar radiation (such as in canopy gaps or due to sunflecks in a forest context) on temperature measurements remain to be quantified. When solar radiation hits the optical fiber cable, it may affect the temperature process by heating the surface of the cable itself, thereby biasing the measurements of ambient air temperatures. Compared to traditional methods that use a cover or (ventilated) radiation shield over the sensor to minimize the influence from sun radiation, it is hard to implement similar methods with DTS over large distances. Therefore, we here study the effect of direct solar radiation on the fiber optic cable to find ways to mitigate the consequences.

## 2. THERMAL EFFECTS OF SOLAR RADIATION ON OPTICAL FIBER CABLES

In this section, we model the optical fiber cable under solar radiation with a solar irradiance of approximately  $1050 \text{ W/m}^2$ , reflecting the typical direct beam radiation on a horizontal surface under cloudless summer conditions with a zero zenith angle [4]. Consider fiber as a cylindrical object where only the cross-sectional area is exposed to solar radiation; if the solar radiation is fully absorbed, the absorbed power can be expressed as:

$$P_{\text{absorbed}} = 1050 \text{ W/m}^2 \times L \times 2 \times R \quad (1)$$

where  $L$  is the length of the fiber we considered here and  $R$  is its radius of fiber. The cylinder will also dissipate heat to the environment. For a concise approximation, we apply Newton's law of cooling:

$$P_{\text{dissipated}} = h \times (T - T_0) \times L \times 2\pi \times R \quad (2)$$

Where  $h$  is the heat transfer coefficient,  $T$  is the temperature of the cylinder, and  $T_0$  is the ambient temperature. When the fiber reaches thermal equilibrium, the absorbed power equals the dissipated power:

$$P_{\text{absorbed}} = P_{\text{dissipated}} \quad (3)$$

The coefficient  $h$  ranging from  $10$  to  $100 \text{ W/K/m}^2$  per a natural or free convection. The temperature increase  $(T - T_0)$  is approximately  $33.4 \text{ }^\circ\text{C}$ . If  $h$  is  $100 \text{ W/K/m}^2$ , the temperature increase is about  $3.3^\circ\text{C}$ . Therefore, the temperature rise ranges from  $3.3 \text{ }^\circ\text{C}$  to  $33.4 \text{ }^\circ\text{C}$ .

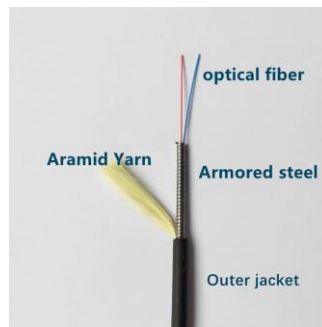


Figure 1. The structure of an armored cable employed for optical-fiber-based distributed temperature sensing.

## 3. FIELD EXPERIMENT

We employ a dual channel 2-km DTS (N4586A-R02, AP Sensing [5]) to measure the temperature along the fiber in our field experiment in National Park Bosland, Belgium ( $51.1623^\circ \text{ N}$ ,  $5.3169^\circ \text{ E}$ ). The spatial resolution is set to  $0.50 \text{ m}$ , which is the smallest distinguishable distance between temperature points, and the sampling resolution is set to  $0.25 \text{ m}$ , to achieve the highest sampling density. The base sampling time of measurement is set to be  $30\text{s}$ , and a  $900\text{s}$  rolling averaging is employed to reduce the unwanted noise in the temperature data.

A 2-km armored cable was deployed in the setup (Fig. 1). We used armored fiber to prevent damage from rodents or other animals. The cable consists of an outer jacket, aramid yarn, armored steel, and a 50/125 multimode optical fiber, as shown in Figure 1. For our setup, different from the sample shown in Figure 1, the cable we are using has only one optical fiber. The outer jacket of the fiber is black. Without interfering with the temperature sampling within the forest, we created an experimental setup using the segment of the fiber closest to the instrument, as shown in Figure 2. This experiment consists of two different fiber regions, each  $50 \text{ cm}$  long, located at positions where the fiber center is at  $14 \text{ meters}$  and  $15 \text{ meters}$ , respectively. At the  $14\text{-meter}$  position, we applied a layer of varybond Alu-Spray (component: aluminum powder  $< 10\%$  [6]) to coat the fiber with an aluminum coating, hence referred to as the Coated region. We use aluminum because aluminum offers greater than  $86\%$  reflectance from near UV to mid IR ( $0.2 - 20 \mu\text{m}$ ), which covers most of the spectrum of the solar radiation [7]. At the  $15\text{-meter}$  position, we kept the fiber in its original state, referred as the Uncoated region. Data was collected on August 28, 2024, covering the period from  $02:00$  to  $22:00$  Central European Time. Direct sunlight exposure occurred between  $10:00$  to  $10:30$ ,  $11:40$  to  $12:10$ , and  $12:30$  to  $14:30$ . At other times, there was diffuse reflection from the surrounding forest.

Due to the proximity of the segments, during the pre-sunrise phase (02:00 to 6:00), until direct sunlight exposure, the temperature difference between the Coated and Uncoated regions was less than 1°C (Fig. 3). This may be due to the aluminum coating reflecting more infrared radiation from the environment, even during nighttime.



Figure 2. Experimental setup in National Park Bosland, Belgium (51.1623° N, 5.3169° E); both the Coated and Uncoated regions are in the indicated while rectangle; the white is coated with aluminum spray, and the black remains the original.

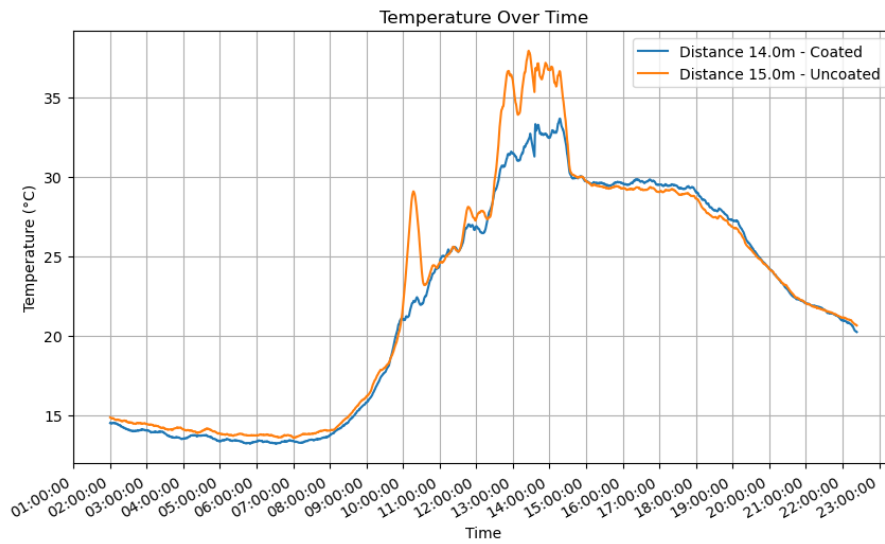


Figure 3. Diurnal temperature cycle of the Coated and Uncoated region of fiber over time from 02:00 in the morning to 22:30 at night on Aug. 28, 2024.

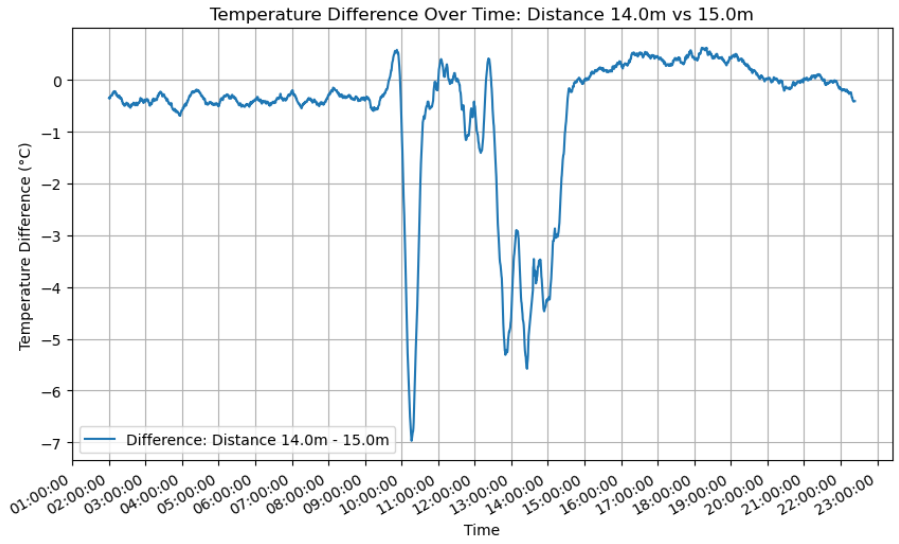


Figure 4. The temperature difference between the Coated and the Uncoated regions of fiber over time from 02:00 to 22:30; negative values indicated that the Coated region of the fiber recorded cooler temperatures than the Uncoated region.

From 10:00 to 10:30, we can observe a rapid increase in the temperature measured by the Uncoated region. In contrast, the temperature rise curve of the Coated region is steady. According to Figure 4, the temperature difference can reach 7 °C. Subsequently, due to the shading from surrounding buildings, the Coated and Uncoated regions are no longer exposed to direct solar radiation, and their temperature difference reduces to less than 1 °C.

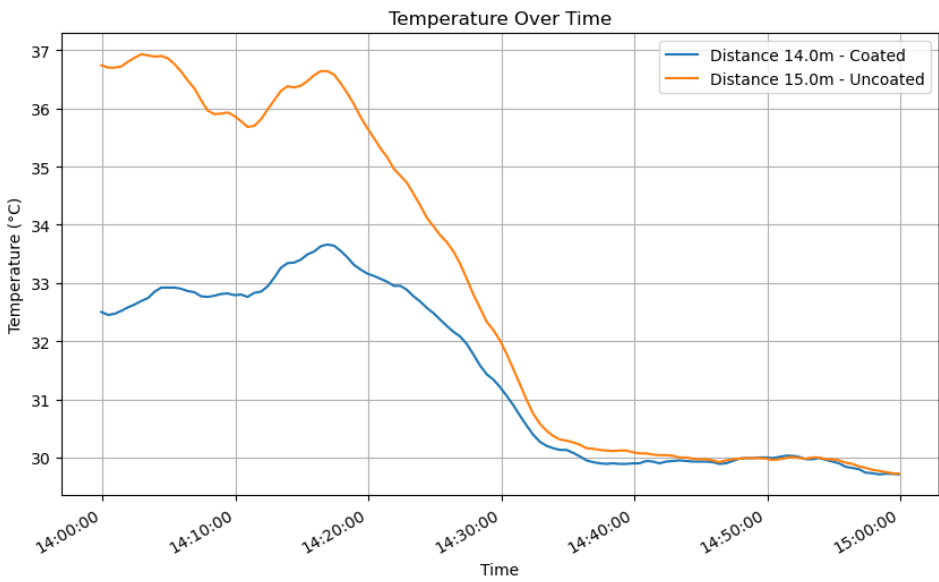


Figure 5. Snapshot of the temperature difference between Coated and Uncoated region of fiber over time from 14:00 to 15:00.

In the absence of direct sunlight (11:00 – 11:30), the Coated and Uncoated regions collected almost identical data, indicating no effect of the aluminum coating on accuracy of air temperature measurements. From 11:30 to 14:30, the fibers were exposed to direct sunlight. During this period, the temperature of the Uncoated region was up to 5 °C higher than that of the Coated region, a thermal increase brought about by energy fluxed from direct solar radiation heating up the black fiber material.

Under solar radiation, we collected temperature readings from 13:00 to 14:00 for averaging. For the Uncoated region, the average temperature is 36.2 °C, while for Coated fiber, it is 32.1 °C. Under the same direction sunlight conditions, the Coated region was 4.1 °C lower than the Uncoated region over the averaging period. Based on this analysis, we believe that the aluminum coating partly mitigates the effect of solar radiation on fiber-based distributed temperature sensing.

#### 4. CONCLUSION

Accurate temperature sensing is critical for understanding the microclimate within a forest. As a promising method, optical-fiber-based temperature distributed sensing provides a flexible method on monitoring the air temperature over a large area with an ultra-fine spatial grain size. However, its sensitivity to temperature also limits its accuracy under direct solar radiation since the readout may deviate from ambient air temperatures because of the fiber's absorption of solar radiation. In this paper, we modeled the solar radiation's effect on the temperature change of distributed sensing cable and conducted a field experiment. Our estimation showed that the temperature of the fiber could increase around 3.3 °C to 33.4 °C. In the setup under direct sunlight, we observed the temperature change on fiber. To reduce the effect of temperature rise of fiber under solar radiation, we also applied an aluminum spray coating to the fiber. The result shows that the temperature of uncoated fiber was 4.1 °C higher than the coated fiber under the same condition. We believe that the aluminum coating on sensing cable is a promising solution to reduce the thermal effect of solar radiation on optical-fiber-based distributed temperature sensing.

#### REFERENCES

- [1] Sanczuk, P., De Pauw, K., De Lombaerde, E., Luoto, M., Meeussen, C., Govaert, S., Vanneste, T., Depauw, L., Brunet, J., Cousins, S., Gasperini, C., Hedwall, P. O., Iacopetti, G., Lenoir, J., Plue, J., Selvi, F., Spicher, F., Uria-Diez, J., Verheyen, K., and Frenne, P., "Microclimate and forest density drive plant population dynamics under climate change," *Nature Climate Change*, vol. 13, pp. 1-8, 2023. doi: 10.1038/s41558-023-01744-y.
- [2] Cannon, J. B., Warren, L. T., Ohlson, G. C., Hiers, J. K., Shrestha, M., Mitra, C., Hill, E. M., Bradfield, S. J., and Ocheltree, T. W., "Applications of low-cost environmental monitoring systems for fine-scale abiotic measurements in forest ecology," *Agricultural and Forest Meteorology*, 321, 108973 (2022). 7 May 2022. <http://doi.org/10.1016/j.agrformet.2022.108973>
- [3] Yu, X., Ergun, K., Cherkasova, L., and Rosing, T. Š., "Optimizing Sensor Deployment and Maintenance Costs for Large-Scale Environmental Monitoring," *IEEE Transactions on Computer-Aided Design of Integrated Circuits and Systems*, vol. 39, no. 11, pp. 3918-3930, Nov. 2020. doi: 10.1109/TCAD.2020.3012232.
- [4] "Introduction to Solar Radiation," Newport Corporation. Available: <https://www.newport.com/t/introduction-to-solar-radiation>. [Accessed: 11-Aug-2024].
- [5] "DTS N45-Series," AP Sensing. Available: <https://www.apsensing.com/technology/dts-n45-series>. [Accessed: 11-Aug-2024].
- [6] "Varybond Alu-Spray Safety Data Sheet," ITW CP Deutschland GmbH. Available: [https://www.itwcp.de/product-184161VAR-en.html?file=t1\\_files/downloads/varybond/spezialsprays/MSDS%20GHS%20EN/VB\\_84\\_Aluspray\\_GB-en\\_2021-03-17.pdf](https://www.itwcp.de/product-184161VAR-en.html?file=t1_files/downloads/varybond/spezialsprays/MSDS%20GHS%20EN/VB_84_Aluspray_GB-en_2021-03-17.pdf). [Accessed: 11-Aug-2024].
- [7] "Coatings | Bare Aluminum," Rocky Mountain Instrument Co. Available: <https://rmico.com/bare-aluminum>. [Accessed: 11-Aug-2024].